November 1999 • NREL/CP-520-27524

Conference Paper

Impurities and Defects in Photovoltaic Si Devices: A Review

Preprint

B. Sopori

To Be Presented at the 10th International Workshop on the Physics of Semiconductor Devices
Delhi, India
December 13, 1999

National Renewable Energy Laboratory

1617 Cole Boulevard
Golden, Colorado 80401-3393

NREL is a U.S. Department of Energy Laboratory
Operated by Midwest Research Institute • Battelle • Bechtel

Contract No. DE-AC36-98-GO10337

Impurities and Defects in Photovoltaic Si Devices: A Review

Bhushan Sopori
National Renewable Energy laboratory
1617 Cole Boulevard
Golden, Co 80401

ABSTRACT

The performance of commercial photovoltaic Si devices is strongly controlled by the impurities and defects present in the substrates. A well-designed solar cell processing sequence can mitigate their effects to yield high efficiency devices. Such a process-design requires a comprehensive knowledge of the properties of defects, impurities, and impurity-defect interactions that can occur during device processing. This paper reviews the recent understanding of the impurity and defect issues in Si-photovoltaics.

INTRODUCTION

The photovoltaic silicon (PV-Si) industry uses both single- and multi-crystalline (mc) wafers that are grown by techniques specially developed to produce low-cost material. Typically, the single crystal ingots are grown by a Czochralski (CZ)-type process, and mc-Si is either cast or in the ribbon form. Because the substrate cost must be kept low, the PV industry employs a host of cost-cutting measures that include low-quality poly feedstock, a lower degree of cleanliness and control in the crystal growth process, and a high crystal-growth rate. These cost-cutting measures compromise the crystallinity as well as the chemical purity of the material. Concomitantly, the PV-Si has high concentrations of impurities and defects [1].

A major goal in solar cell fabrication is to be able to design process schedules that can minimize the deleterious effects of the impurities, defects, and (or) passivate them [2-4]. Indeed, it is possible to design cell processing steps that can accomplish a significant reduction in the dissolved impurity concentrations and produce favorable impurity/defect interactions as a byproduct. Such processes have led to commercial Si solar cells with efficiencies of 14-15%. However, further improvements in the device performance requires using new concepts that can mitigate the deleterious effects resulting from impurity-defect interactions during crystal growth and device fabrication.

This paper reviews the basic behavior of impurities and defects in Si. We show that impurity-defect interactions play an important role in determining the performance of silicon PV devices, and it is necessary to know such interactions to design processes that can mitigate their detrimental effects on the device performance.

IMPURITIES AND DEFECTS IN PV-Si

Si-PV manufacturers use low-grade feedstock consisting of pot-scrap, off-spec, and remelt—much of this material is the reject from the microelectronic industry. The impurities present in the feedstock are carried into the melt and into the grown crystal dictated by the segregation coefficients. Hence, in general, the PV starting material has a high impurity content. Typically these substrates contain C and/or O in near-saturation levels, transition metals in the range of 10^{12}-10^{14} cm^{-3}, and a host of other impurities such as Ti and Va.

Because of their high concentrations, in many cases impurities can precipitate at preferred sites such as extended defects, grain boundaries, and defect clusters. The chemical structure of such precipitates can be quite complex. For example, micro-X-ray analyses have shown that some precipitates are predominantly metallic but have significant amounts of oxygen and or carbon associated with them. This may indicate that metal precipitates are silicides, carbides, and oxides. On the other hand, this may mean that metal precipitation is a secondary process that takes place in the proximity of pre-existing oxygen/carbon precipitates. Such a phenomenon may occur as a local stress relaxation mechanism.

The single-crystal CZ ingots for PV are pulled at growth rates that can be many times faster than that of the conventional growth for microelectronics. These fast cooling rates are accompanied by excessive thermal stresses that lead to generation of defects. Consequently, the single crystal material is expected to have high concentrations of quenched-in, non-equilibrium, point defects. In some cases, a portion of the ingot may acquire a high density of crystal defects (primarily dislocations) and even lose the crystallinity and become multicrystalline. The mc-Si substrates typically consist of very large grains with a small grain boundary area producing only a small effect on the device performance. The dominant intragrain defect is dislocation. High-quality mc-Si substrates have a tendency to form clusters of defects. Figure 1 is a map of a typical, 4.25-in x 4.25-in, commercial, multicrystalline PV-Si wafer. The wafer has an average defect density of about $10^{5}cm^{-2}$; however, as seen in the figure, there are localized clusters of defects where the defect density can exceed $10^{7}cm^{-2}$. Our previous work has shown that such defects consist of networks of dislocations, stacking faults and grain boundaries. Detailed analyses have shown that such defect clusters are sites of impurity precipitates. Figure 2 shows a TEM photograph of precipitates at a defect cluster. It is rather interesting that impurity precipitation occurs at defect clusters rather than at grain boundaries and other isolated defects [1].

Wafers of mc-Si exhibit a preponderance of twins. The most commonly observed twins are coherent twin-lamelli that have a (111) twinning plane. A high-quality wafer may have 20–30% of the area covered by such twins. These regions are generally free of dislocations and constitute the best quality material in a wafer. In addition to the coherent twins, the wafers have higher order twin boundaries, which are often decorated with dislocations.

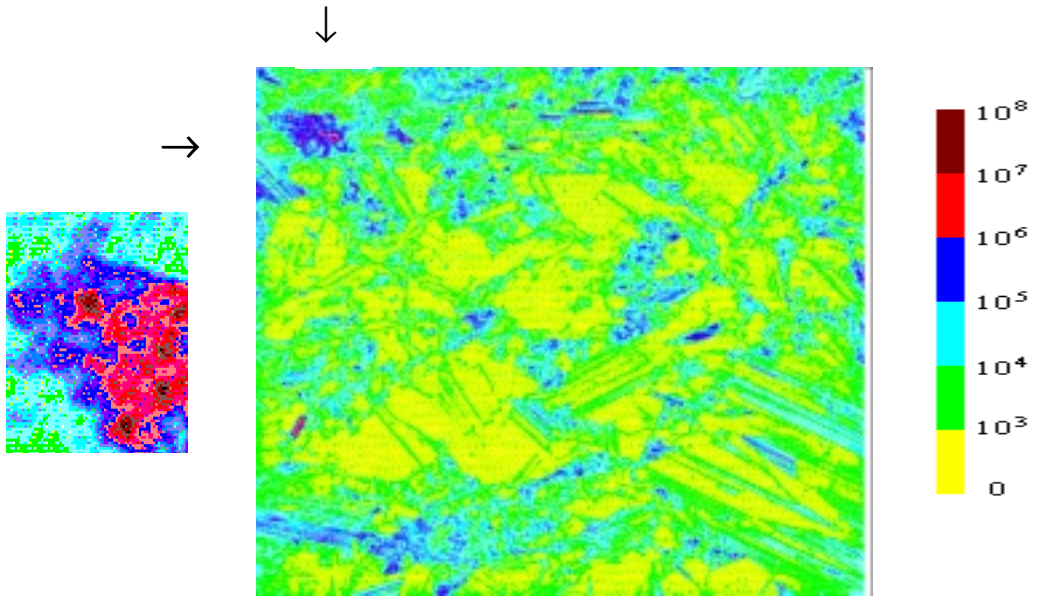

Figure 1. Dislocation density map of a commercial 4.25-in x 4.25-in mc-Si wafer. The numbers in the legend indicate dislocation density in cm^{-2}. The inset on the left shows a magnified view of the region indicated by the arrows.

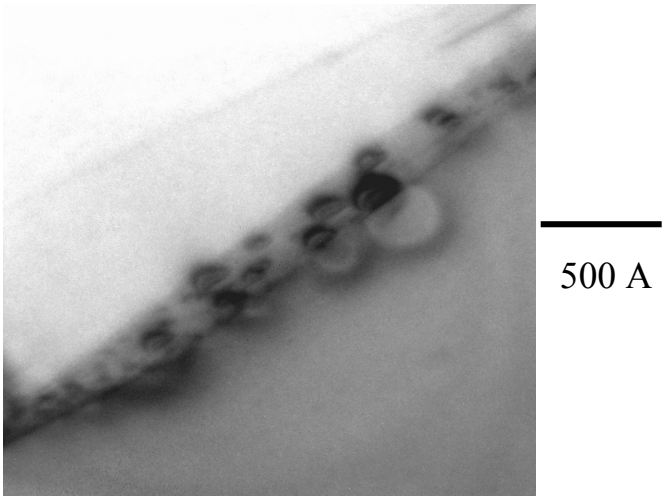

Figure 2. A TEM photograph showing impurity precipitation at a defect cluster site. μ–X-ray analyses shows that the precipitates have many elemental impurities.

RECOMBINATION CAUSED BY IMPURITIES AND DEFECTS

Impurities and defects introduce energy levels in the bandgap with a concomitant increase in the minority-carrier recombination. The impurities of most interest in PV-Si are the transition metals (TM), particularly Fe, Cr, and Ni. In the dissolved state, these impurities are highly mobile with diffusivities close to 10^{-6} cm^2 s^{-1}, and they produce deep levels. Typically, the total concentration of the TM is quite high, near $10^{14}cm^{-3}$. It is fruitful to consider some details of their recombination properties in Si. We can use Fe as an example; other metals have a somewhat similar behavior. In the past thirty years, Fe in Si has been studied extensively, both

experimentally and theoretically [5,6]. Iron exists in Si in two forms: as interstitial and as a complex with other defects. At room temperature, the interstitial iron (Fe_i) introduces a donor level at $E_T \approx E_V+(0.375\pm0.015)$ eV. The hole capture cross-section of interstitial iron can be written as (in cm^{-2}):

$$\sigma_p(Fe_i) = (3.9 \pm 0.5) \times 10^{-16} \times \exp(-\frac{0.045 \pm 0.005 eV}{k_B T})$$

where k_B stands for the Boltzman constant, and T is the temperature. The electron capture cross-section of Fe at room temperature was measured as $\sigma_n = 4\times10^{-14}$ cm^{-2}. Because of near-mid gap energy and a large capture cross section, it is expected that Fe will produce high recombination or low minority-carrier lifetime.

The interstitial iron in p-Si is positively charged at room temperature and at slightly elevated temperatures. As a result, it tends to form pairs with negatively charged defects, such as shallow acceptors. More than 30 complexes can be formed between iron and other defects, and about 20 deep levels are associated with these complexes. The positions of these energy levels vary from about Ev+0.07 eV to Ec-(0.26±0.03) eV. They could be either donor levels or acceptor levels. The hole capture cross section ranges from $3.9\text{x}10^{-16}$ to $2\text{x}10^{-13}$ cm^{-2}, while the electron capture cross section can change from $1.5\text{x}10^{-16}$ to $4\text{x}10^{-13}cm^{-2}$. Of particular interest is the ability of Fe to form complexes with two major impurities in Si-B and O. The B-Fe forms a donor level at E_v+0.1 eV ($\sigma_n = 4\times10^{-13}$ cm^{-2} at the room temperature) and an acceptor level at E_c-0.29 eV. The recombination rate caused by the Fe-B pair is lower than that of interstitial Fe at low injection levels. The formation of Fe-B is an important effect that has an implication on solar cell technology. Fe-B recombination has a more pronounced effect in lower resistivity P-type Si. At lower temperatures, nearly all Fe present in a Si wafer occurs as Fe-B. In a B-doped PV-Si wafer containing Fe, the recombination can be further increased by the presence of defects. Figure 3a shows the minority carrier diffusion length (MCDL) as a function of Fe concentration in a PV-Si wafer. The solid line is the calculated curve for Fe-B limited recombination, while the crosses indicate experimental data measured by an SPV technique. It is clear that the MCDL is lower than the Fe-B limit, and one may envision two groups of MCDL values identified by numerals I and II that may correspond to two types of defects. Figure 3b shows the measurements on the same wafer after a P-diffusion for impurity gettering. This figure shows that defects associated with group II were gettered, leading to an increase in the MCDL, while that of group I remained mainly unaltered. A discussion of this feature is given later in this paper.

It should be pointed out that Fe-B complexes dissociate at temperatures of about 200°C or by illumination of high intensity light (typically about a few W/cm^2). A dissociation of Fe-B results in an increase in the recombination and a decrease in τ. It has also been known for a while that the values τ in low-resistivity, B-doped substrates are much lower than one can expect on the basis of impurity scattering by B concentration alone. Recent studies have shown that Fe-B pair formation is responsible for a rapid decrease in the resistivity (in B-doped material). It is important to recognize that in a solar cell many impurities are gettered during the cell fabrication. Thus, the behavior of many impurities is quite dynamic in solar cell material.

Recent studies have also shown that Fe-O pair formation occurs in some solar cells. This effect is manifested as a decrease in the MCDL on illumination of the cell under sunlight. This mechanism produces a pronounced effect of reducing the efficiency of a Si solar cell.

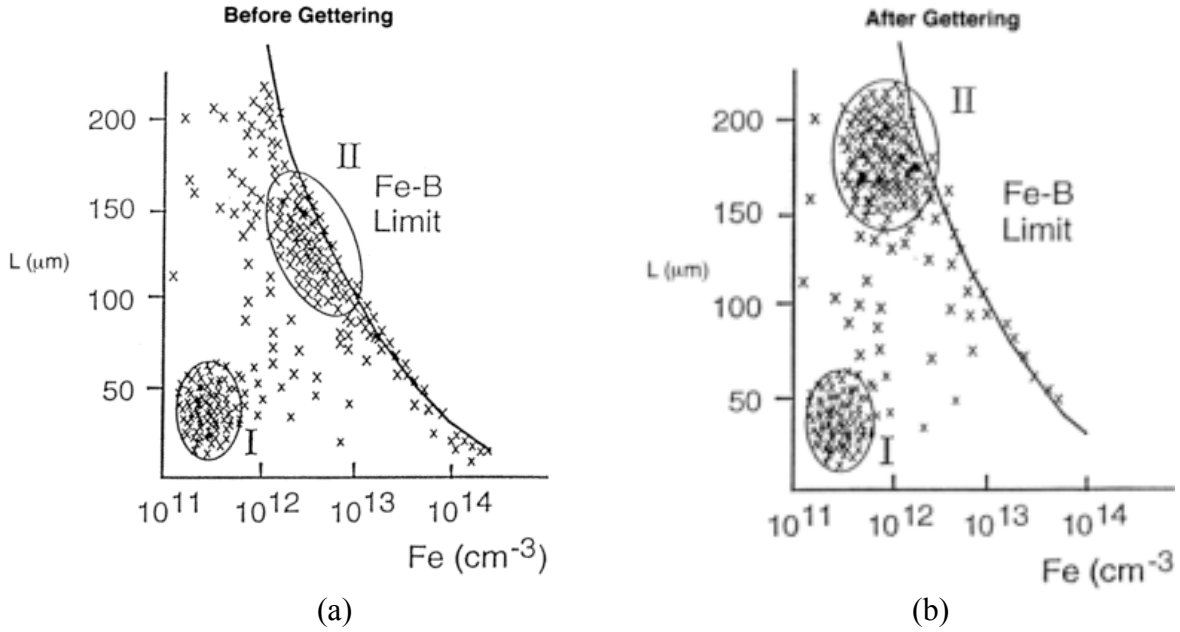

Figure 3. Minority-carrier diffusion length as a function of dissolved Fe concentration —(a) as-grown material, and (b) P-diffusion.

Like impurities, defects introduce energy levels in the bandgap. The nature of the levels in a real material is quite complex because the defects represent a host of defect configurations. Crystal defects always appear to have detrimental effects on the material quality. Defects are discontinuities in the periodic lattice with associated dangling bonds —they introduce bandgap states. Electronic properties of defects have been studied for decades. Here we show how the non-uniformities created by the distribution of defects influences the recombination behavior of Si-PV wafers. Figure 4a, 4b, and 4c show room-temperature photoluminescence, defect distribution, and MCDL maps of a 2-in x 2-in Si wafer. We see that recombination characteristics are strongly controlled by the defects.

Although a great deal of understanding has been achieved based on the experimental results, a characteristic feature of various experimental investigations is a lack of reproducibility of the results. The reason is very simple – in a real material each defect can be different and each defect can exhibit different properties at different parts of the same defect. One of the major reasons for this is that the properties of defects are very sensitive to impurities in the material. This is because the interactions between defects and impurities occur very readily. As an

example, Figure 5 shows the MCDL of Si as a function of dislocation density for different resistivity materials. The effect of dislocations is strongly dependent on the resistivity of the substrate.

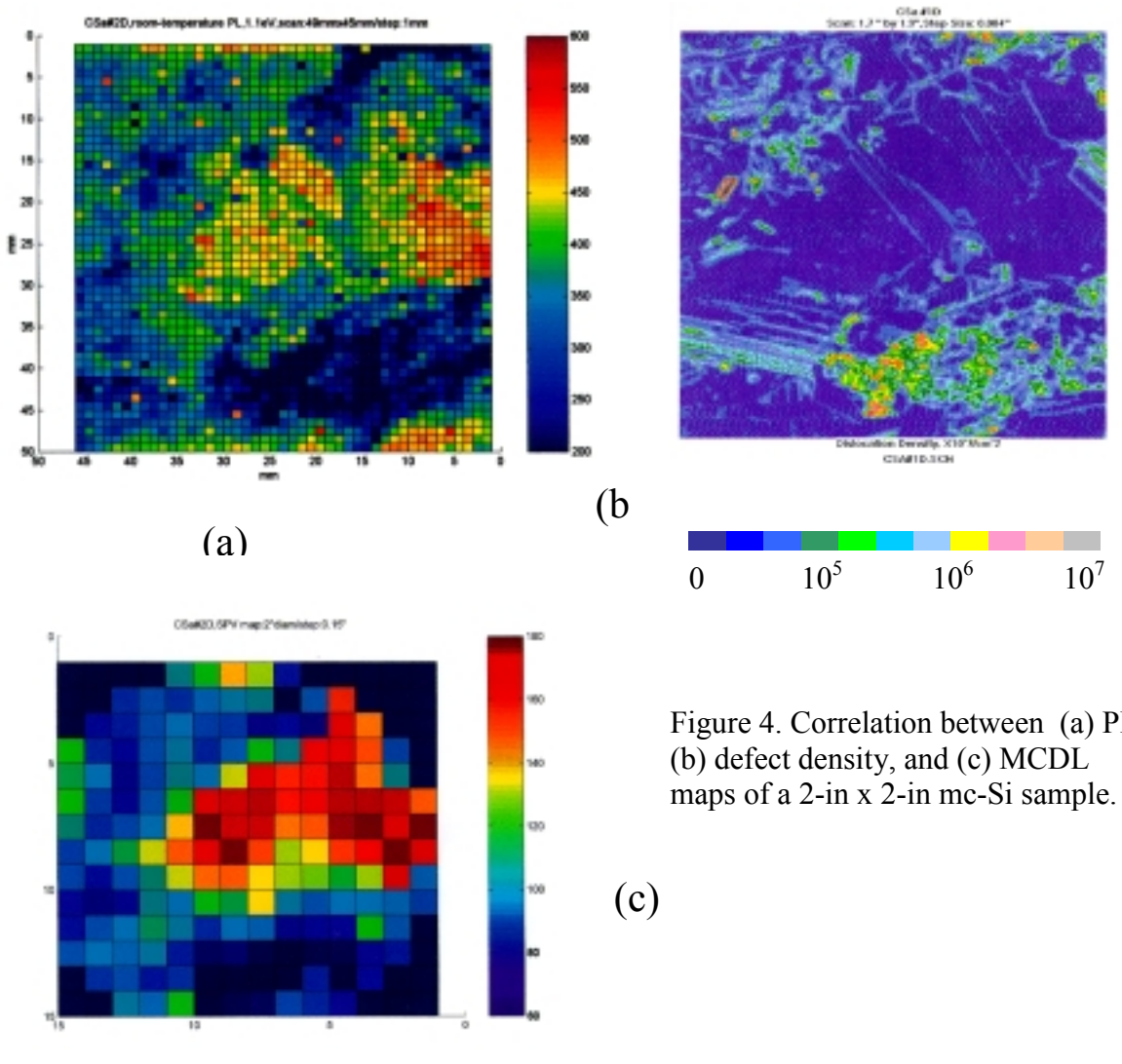

Figure 4. Correlation between (a) PL, (b) defect density, and (c) MCDL maps of a 2-in x 2-in mc-Si sample.

REMOVAL OF IMPURITIES FROM Si

It is well known that the performance of solar cells would be quite poor if the device had as high concentrations of impurities as in the as-grown PV-Si. Fortunately, some of the impurities are removed during the device processing. This mechanism, called gettering, has been used in microelectronic devices to trap impurities away from the active region of the device by oxygen

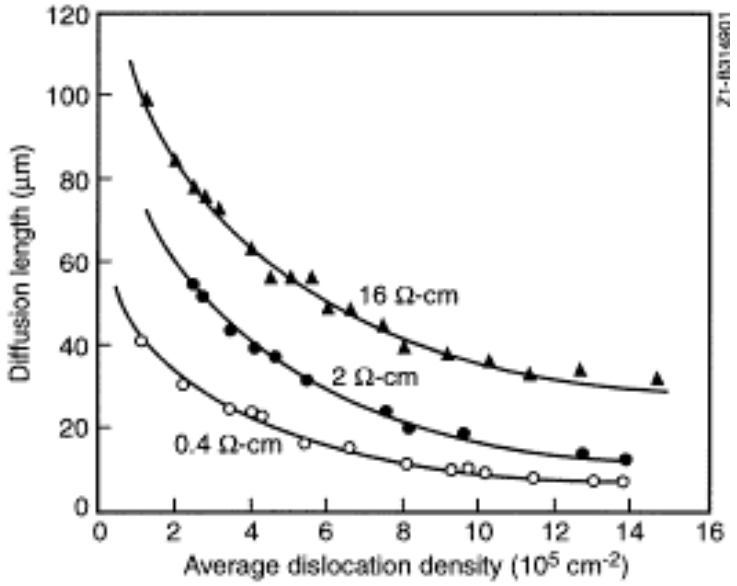

Figure 5. Dependence of the minority carrier diffusion length on the dislocation density fro different resistivity

precipitates. Solar cells, being minority-carrier devices, use nearly the entire bulk of the device. Hence, it is more attractive to apply external gettering techniques to clean up the bulk of the material. Phosphorous diffusion and Al alloying are some of the processes that have worked well for efficient gettering of solar cells. Because these processes are extensively used in solar cell manufacturing for junction and contact formation, all Si solar cells experience a certain degree of gettering. However, it is often necessary to optimize each of these process steps such that the highest degree of gettering is attained without sacrificing the junction or the contact properties.

Because the difusivities of the TM is quite high, typically 10^{-6} cm^2s^{-1}at the typical process temperatures, these impurities can diffuse out very rapidly during a gettering process. Figure 6 shows the gettering effect in a multicrystalline Si wafer produced by a P-diffusion at 850°C. The results are shown as the MCDL before and after gettering. It is seen that the average MCDL increases 40 μm to 65 μm; however, not all the regions experience an increase in the MCDL.

As expected, effective gettering of TM impurities can be achieved using conventional solar cell fabrication process steps, if the impurities are in the dissolved state. However, as indicated earlier in this paper, many impurities precipitate at the defect clusters. To getter the precipitated impurities, the precipitates must be dissolved before the impurities can become mobile. Unfortunately, impurity dissolution is a very slow process at reasonable process temperatures. Such a dissolution depends on the temperature as well as the precipitate size.

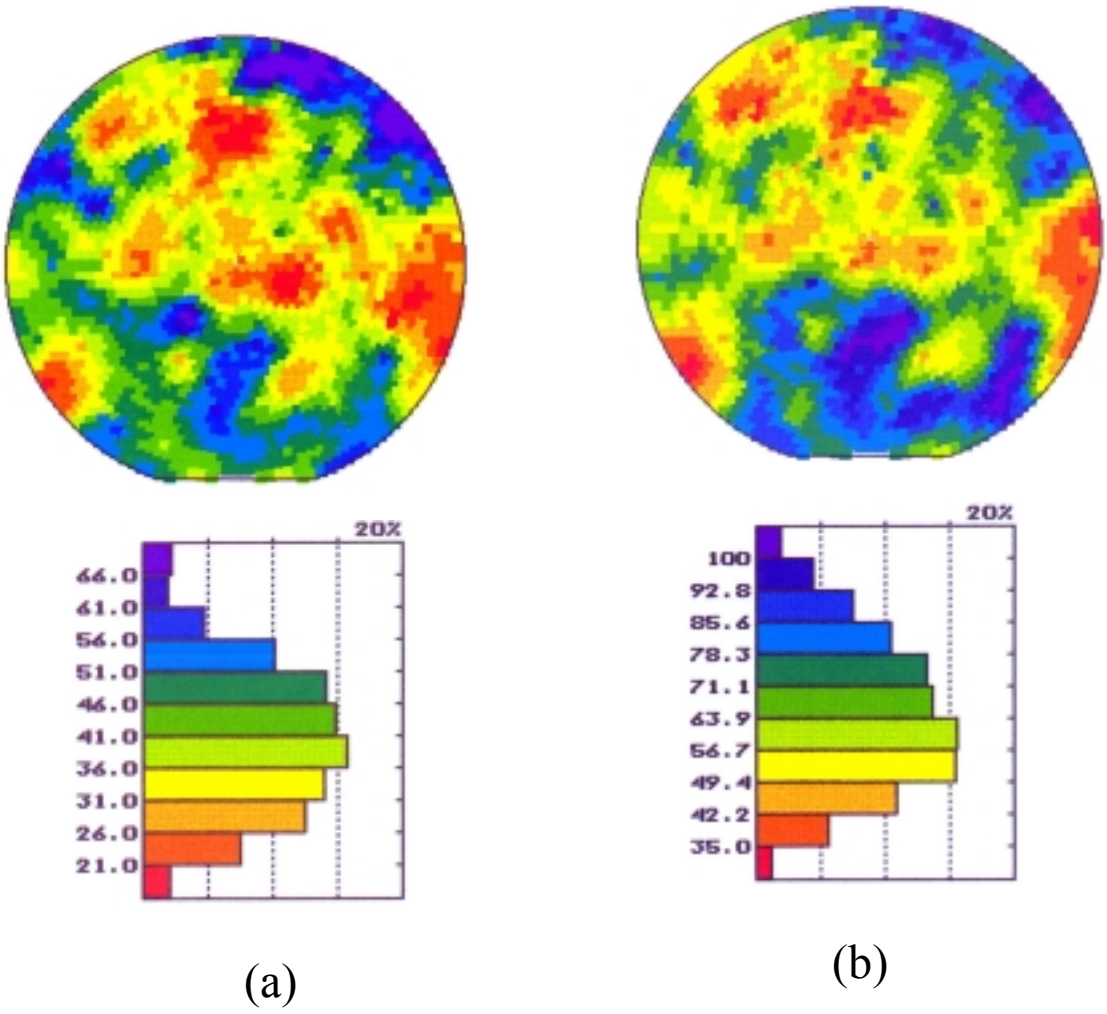

Figure 6. Comparison of the minority carrier diffusion length before (a) and after P gettering (b).
Gettering: 850°C, 15 min

Again, we can use Fe as the "test" impurity to study the gettering behavior resulting from an Al alloying process. Typically Al alloying is done at 800ºC, using 1 μm of Al. We consider a 300-μm-thick wafer having a dissolved Fe concentration of 10^{14} cm^{-3}, and examine changes in the total Fe, integrated within the thickness of the wafer, as a function of gettering time (on a normalized scale). Figure 7 shows these results for three cases — (a) Fe dissolved to a concentration of 10^{14} cm^{-3} without any precipitates, (b) additional precipitates, 6 nm in diameter as a silicide, concentration of 10^{11} cm^{-3} (which adds about $5x10^{11}$ cm^{-3} Fe atoms in precipitated form , and (c) precipitates 50 nm in size.

It is seen that in case (a) the Fe concentration will reduce by two orders of magnitude in 30 min. and by three orders in 60 min. In case (b), because the dissolved Fe atoms are supersaturated at 800ºC, the precipitates grow rapidly at the beginning of gettering. However, gettering of Fe atoms to the gettering layer becomes very ineffective, and its effect will be noticed only after a substantial amount of time so that effective precipitate dissolution has occurred. For the Al gettering process at 800^{o}C, it will now take more than 7 hr to reduce the total Fe concentration by three orders. For larger precipitates, case c, still longer gettering times are needed; e.g., for the precipitate size of 50 nm it will take many days at 800^{o}C to notice any gettering effect [7]. We expect that a similar situation holds also for Cr, but only more difficult, because of its lower (one order of magnitude) diffusivity value.

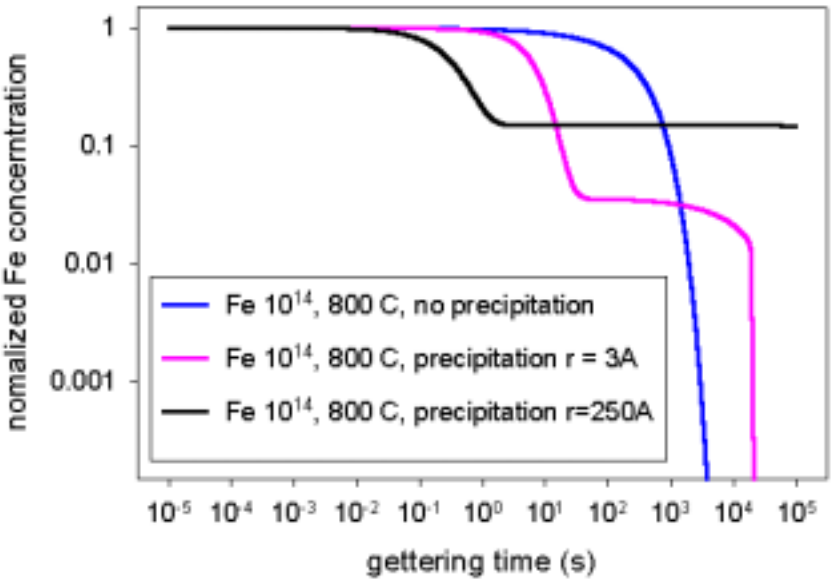

Figure 7. Normalized, total Fe concentration in a 300-μm thick Si wafer (as a function of gettering time) for various conditions of dissolved and precipitated Fe. Precipitated Fe is assumed to be an Fe silicide.

These results clearly show that gettering of defect clusters (that have precipitated impurities) can be very difficult, and that conventional processing techniques can not dissolve the impurities within such regions. It is important to note that while the majority of the substrate may experience an effective gettering, the local regions of defect clusters remain effectively unchanged. Figure 8 illustrates this feature. Figure 8a is a photoresponse map of a solar cell and Figure 8b is its defect map. It is seen that high defect density regions have very poor photoresponse because of very high recombination. In a large-area device the local regions of high recombination can lead to "shunts" that can severely degrade the voltage-related device parameters. The next section shows that these regions can strongly limit the device performance.

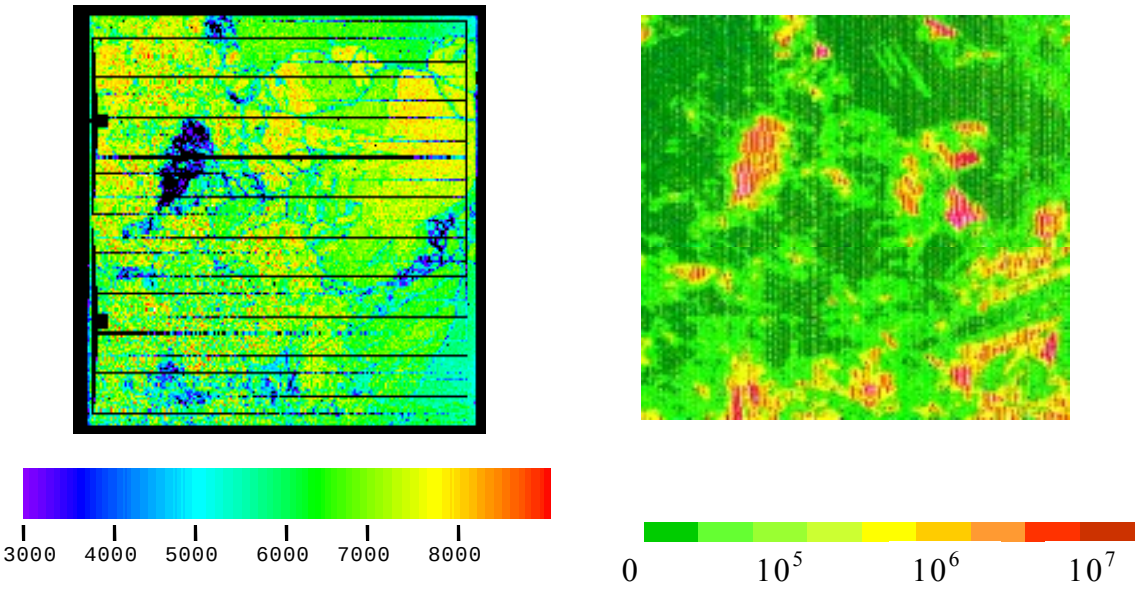

Figure 8. (a) A photoresponse map of a solar cell taken with a long wavelength excitation showing the bulk response of the device. The defect map of the device is shown in (b). The scales are in counts and defects cm^{-2}, respectively.

THE INFLUENCE OF DEFECTS AND IMPURITIES ON THE DEVICE PERFORMANCE

As discussed above, presence of impurities and defects makes a solar cell a non-uniform device. In the previous section, we have already seen that defects and impurities can lower the MCDL in the as-grown substrate. Predicting the effect of impurities and defects on the device performance is, however, quite difficult [8]. A quantitative investigation of the effect of defects on the cell performance can be performed using a phenomenological approach that involves the following steps:

1. Determine the characteristics of the cell with no defects
2. Determine the characteristics of the cell corresponding to the defect cluster region, and
3. Combine the above two to form a distributed device having a given distribution of defect clusters.

Item 1 is straightforward and can be expressed in a standard form as:

$J_{dark}(V) = J_{01}.\exp.\{ (-eV/kT) - 1\} + J_{02}.\{ \exp. (-eV/2kT) - 1\}$

The saturation currents J_{01}.and J_{02} can be written as:
$J = J_{ph} - J_{dark}(V)$, where J_{ph} and $J_{dark}(V)$ are the photogenerated and the dark current densities, respectively.

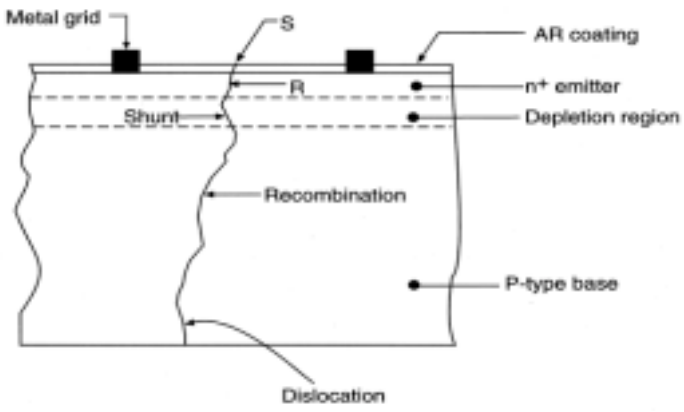

Figure 9. A schematic illustrating recombination due to defects in a PN junction device

A similar formalism can be applied to the local, defected region of a solar cell [3]. Because defects can propagate in different regions of the device (see Figure 9), one must consider their influence on the base as well as the junction regions. We have shown that the defected region can also be represented by equations similar to 1 and 2 above. However, in this case the values of various parameters will be different. We have developed a computer model for an N/P junction device that calculates these parameters and uses a distributed network model to combine various regions of the device.

The device is divided into an array of diodes, each diode is small enough to assume a uniform distribution of defects. Each node in the matrix depicts a local cell, connected to other cells by a resistor representing the series resistance. The series resistance arises from a number of sources that include the sheet resistivity of the junction in an N/P device.

We consider an example of a cell in which 20% of the device area is covered by heavily defected regions, and 80% of the area is defect-free. The parameters for the defect-free region are:

J_{ph}= 0.035A/cm^2, J_{01}= 3.6 x 10^{-9} A/cm^2 , J_{02}= 4.5 x 10^{-13} A/cm^2

From the experimental data, the parameters for the "defected" cell are:

J_{ph}= 0.0245 A/cm^2 , J_{01}= 3.6 x 10^{-8} A/cm^2 , J_{02}= 4.5x 10^{-11} A/cm^2

Figure 10 shows the calculated I-V characteristics of these two cells. Their cell parameters are: {V_{oc}= 650 mV, J_{sc}= 34.45 mA/cm^2, FF= 81.01, and the efficiency=18.4}for defect-free and {V_{oc}= 620mV, J_{sc}=32.7 mA/cm^2, FF= 75.76, Eff = 16.7} for defected cells, respectively. It is seen that all the parameters of the "defected" cell are lower than for the "defect-free" cell. However, the major reduction is in the V_{oc} and the FF. It should be pointed out that in an "undefected" cell , a reduction of 30 mV would be accompanied by a large reduction in J_{sc} in accordance with the cell equation; shunting produces a disproportionate reduction in the voltage.

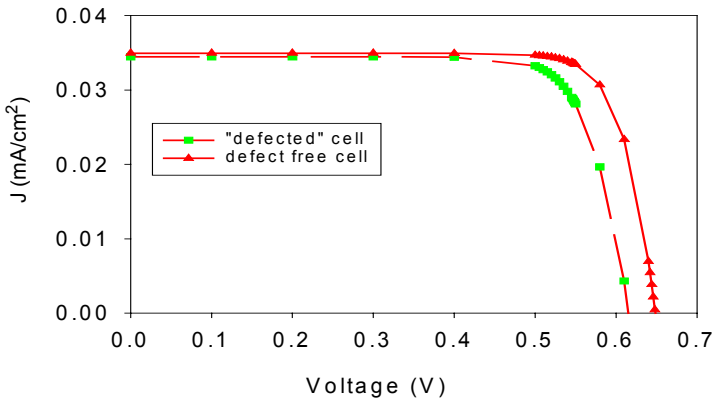

Figure 10. Calculated I-V characteristics of solar cells with and without defects.

It is important to point out that the cell performance depends not only on the number of defects in the substrates but also on how the defects are distributed. To demonstrate this effect, we consider an example of solar cells fabricated on substrates with different distributions of defects and calculate their device parameters. Figure 11 illustrates these distributions and gives cell efficiency for different defect configurations. Table 1 shows a summary of all the cell parameters.

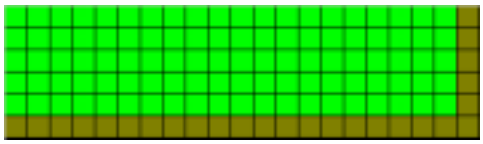

(a) Zero-D, Efficiency=17.6% (for comparison)

(b) 10E6 cm^{-2}, Efficiency=11.1%(for comparison)

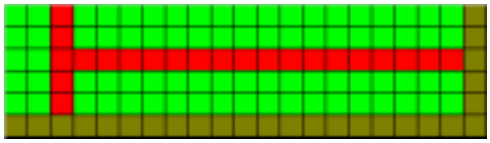

(c) T-distribution 10E6 cm^{-2}, Efficiency=15.5%

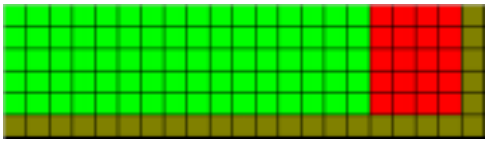

(d) Bar, 10E6 cm^{-2}, efficiency=15.8%

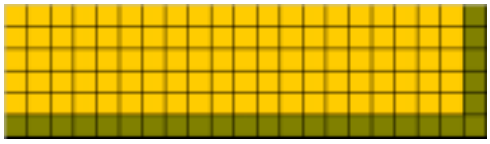

(e) 2x10E5 Uniformly distributed, Efficiency=16.4%

Figure 11. Schematics illustrating the effect of different distribution of defects in a solar cell. The cells in (c), (d) and (e) have the same number of defects.

Table 1. Summary of the solar cell parameters for different distribution of defects

Cell configuration	Efficiency (%)	V_{oc} (mV)	J_{sc} (mA/cm^2)	FF (%)
No defects	17.6	650	34.9	77.6
20% bar	15.8	615	33.2	77.4
20% T	15.5	615	33.2	75.9
Uniform	16.4	650	32.5	77.6
All defects	11.1	565	26.2	75

CONCLUSIONS

We have reviewed some basic properties of impurities and defects in PV-Si devices. Dissolved impurities, particularly TM, can be easily gettered during cell fabrication. Fe is used as an example to show various mechanisms that can influence the carrier recombination behavior in Si. The defect clusters are sites for impurity precipitation, particularly for the metallic impurities. The chemical nature and the precipitate size can play an important role in whether it can be gettered from the device. Thus, it is important to know the chemical composition of the precipitates. Examples are given to show how defects and impurities can influence the solar cell performance. Modeling results are presented to show that both the number and the distribution of defects play an important role in the performance of a solar cell.

ACKNOWLEDGEMENT

The author would like to thank Wei Chen for his help in preparing this manuscript. This work was supported by the US Department of Energy under Contract No.DE-AC36-99GO10337.

REFERENCES

[1] Bhushan Sopori, Procd. ICDS-19, Trans Tech Pub., Edited by Gordon Davies and Maria Helena Nazare, 527 (1997).
[2] B. L. Sopori, L. Jastrzebski, T. Y. Tan, and S. Narayanan, Procd. 12th PVSEC, 1003(1994).
[3] B. L. Sopori, W. Chen, K. Nemire, J. Gee, S. Ostapenko, Procd. 2nd World Conference on Photovoltaic Solar Energy Conversion, Vienna, 152 (1998).
[4] B. L. Sopori et.al , Solar Energy Materials and Solar Cells, 41/42, 159 (1996).
[5] A. A. Istratov, H. Hieslmair, and E. R. Weber, Appl. Phys. **A69**, 13-44 (1999).
[6] Proceedings of the 9th Workshop on Crystalline Silicon Solar Cell Materials and Processes, NREL/BK-520-26941, Edited by B. L. Sopori.
[7] B. L. Sopori, W. Chen, T. Y. Tan, and P. Plekhanov, NCPV Photovoltaics Program Review, AIP Conference Proceedings, **462**, Editors, M. Al-Jassim, J. Thornton, and J. Gee, 341 (1998).
[8] J. G. Fossum and F. A. Lindholm., IEEE Trans. ED-27, 692(1980).

REPORT DOCUMENTATION PAGE

Form Approved
OMB NO. 0704-0188

1. AGENCY USE ONLY (Leave blank)	2. REPORT DATE	3. REPORT TYPE AND DATES COVERED
	November 1999	conference paper

4. TITLE AND SUBTITLE
Impurities and Defects in Photovoltaic Si Devices: A Review

5. FUNDING NUMBERS
C
TA: PV003101

6. AUTHOR(S)
B. Sopori

7. PERFORMING ORGANIZATION NAME(S) AND ADDRESS(ES)

8. PERFORMING ORGANIZATION REPORT NUMBER

9. SPONSORING/MONITORING AGENCY NAME(S) AND ADDRESS(ES)
National Renewable Energy Laboratory
1617 Cole Blvd.
Golden, CO 80401-3393

10. SPONSORING/MONITORING AGENCY REPORT NUMBER
CP-520-27524

11. SUPPLEMENTARY NOTES

12a. DISTRIBUTION/AVAILABILITY STATEMENT
National Technical Information Service
U.S. Department of Commerce
5285 Port Royal Road
Springfield, VA 22161

12b. DISTRIBUTION CODE

13. ABSTRACT *(Maximum 200 words)*
The performance of commercial photovoltaic Si devices is strongly controlled by the impurities and defects present in the substrates. A well-designed solar cell processing sequence can mitigate their effects to yield high efficiency devices. Such a process-design requires a comprehensive knowledge of the properties of defects, impurities, and impurity-defect interactions that can occur during device processing. This paper reviews the recent understanding of the impurity and defect issues in Si-photovoltaics.

14. SUBJECT TERMS
photovoltaics ; silicon ; solar cells ; impurities and defects

15. NUMBER OF PAGES

16. PRICE CODE

17. SECURITY CLASSIFICATION OF REPORT	18. SECURITY CLASSIFICATION OF THIS PAGE	19. SECURITY CLASSIFICATION OF ABSTRACT	20. LIMITATION OF ABSTRACT
Unclassified	Unclassified	Unclassified	UL